AJNR

Application of Spinal Subtraction and Bone Background Fusion CTA in the Accurate Diagnosis and Evaluation of Spinal Vascular Malformations

Xuehan Hu, Zhidong Yuan, Kaiyin Liang, Min Chen, Zhen Zhang, Hairong Zheng and Guanxun Cheng

AJNR Am J Neuroradiol 2024, 45 (3) 351-357
doi: https://doi.org/10.3174/ajnr.A8112
http://www.ajnr.org/content/45/3/351

Application of Spinal Subtraction and Bone Background Fusion CTA in the Accurate Diagnosis and Evaluation of Spinal Vascular Malformations

Xuehan Hu, Zhidong Yuan, Kaiyin Liang, Min Chen, Zhen Zhang, Hairong Zheng, and Guanxun Cheng

ABSTRACT

BACKGROUND AND PURPOSE: Accurate pretreatment diagnosis and assessment of spinal vascular malformations using spinal CTA are crucial for patient prognosis, but the postprocessing reconstruction may not be able to fully depict the lesions due to the complexity inherent in spinal anatomy. Our purpose was to explore the application value of the spinal subtraction and bone background fusion CTA (SSBBF-CTA) technique in precisely depicting and localizing spinal vascular malformation lesions.

MATERIALS AND METHODS: In this retrospective study, patients (between November 2017 and November 2022) with symptoms similar to those of spinal vascular malformations were divided into diseased (group A) and nondiseased (group B) groups. All patients underwent spinal CTA using Siemens dual-source CT. Multiplanar reconstruction; routine bone subtraction, and SSBBF-CTA images were obtained using the snygo.via and ADW4.6 postprocessing reconstruction workstations. Multiple observers researched the following 3 aspects: 1) preliminary screening capability using original images with multiplanar reconstruction CTA, 2) the accuracy and stability of the SSBBF-CTA postprocessing technique, and 3) diagnostic evaluation of spinal vascular malformations using the 3 types of postprocessing images. Diagnostic performance was analyzed using receiver operating characteristic analysis, while reader or image differences were analyzed using the Wilcoxon signed-rank test or the Kruskal-Wallis rank sum test.

RESULTS: Forty-nine patients (groups A and B: 22 and 27 patients; mean ages, 44.0 [SD, 14.3] years and 44.6 [SD,15.2] years; 13 and 16 men) were evaluated. Junior physicians showed lower diagnostic accuracy and sensitivity using multiplanar reconstruction CTA (85.7% and 77.3%) than senior physicians (93.9% and 90.9%, 98% and 95.5%). Short-term trained juniors achieved SSBBF-CTA image accuracy similar to that of experienced physicians ($P > .05$). In terms of the visualization and localization of spinal vascular malformation lesions (nidus/fistula, feeding artery, and drainage vein), both multiplanar reconstruction and SSBBF-CTA outperformed routine bone subtraction CTA ($P = .000$). Compared with multiplanar reconstruction, SSBBF-CTA allowed less experienced physicians to achieve superior diagnostic capabilities (comparable with those of experienced radiologists) more rapidly ($P < .05$).

CONCLUSIONS: The SSBBF-CTA technique exhibited excellent reproducibility and enabled accurate pretreatment diagnosis and assessment of spinal vascular malformations with high diagnostic efficiency, particularly for junior radiologists.

ABBREVIATIONS: AP = arterial phase; AUC = area under the curve; CE-MRA = contrast-enhanced MRA; MPR-CTA = multiplanar reconstruction CTA; RBS-CTA = routine bone subtraction CTA; ROC = receiver operating characteristic; SSBBF-CTA = spinal subtraction and bone background fusion CTA; SVM = spinal vascular malformation; 3D-VR =3D volume-rendering

Spinal vascular malformations (SVMs) are rare CNS vascular lesions, with spinal AVFs (arteriovenous directly shunting with a fistula) and AVMs (arteriovenous connection with a true nidus) being the most common types (95%).[1] Their clinical presentations are variable and nonspecific, including progressive motor, sensory, and urogenital disturbances, similar to chronic myelitis, demyelinating lesions, disc lesions, and so forth.[2,3] However, the treatments and prognoses differ completely. Delayed or incorrect diagnosis and treatment can lead to serious complications, permanent disability, and even fatality.[4-6] Therefore, accurate

Received August 26, 2023; accepted after revision December 2.

From the Department of Radiology (X.H., Z.Y., K.L., Z.Z., G.C.), Peking University Shenzhen Hospital, Shenzhen, China; Paul C. Lauterbur Research Center for Biomedical Imaging (X.H., H.Z.), Shenzhen Institutes of Advanced Technology, Chinese Academy of Sciences; and Department of Radiology (M.C.), Southern University of Science and Technology Hospital, Shenzhen, China.

Xuehan Hu and Zhidong Yuan contributed equally to this work and should be considered co-first authors.

This work was supported by the China Postdoctoral Science Foundation (No. 2021M703373) and the Shenzhen High-Level Hospital Construction Fund.

Please address correspondence to Guanxun Cheng, MD, PhD, Peking University Shenzhen Hospital, 1120#, Lianhua Rd, Futian District, Shenzhen, 518036 Guangdong, China; e-mail: chengguanxun@outlook.com

Indicates article with online supplemental data.

Indicates article with supplemental online video.

http://dx.doi.org/10.3174/ajnr.A8112

diagnosis and evaluation before treatment are crucial for developing an appropriate treatment plan and improving neurologic function.

Spinal DSA is the criterion standard for diagnosing SVMs.[7,8] However, selective level-by-level radicular spinal DSA is technically difficult, particularly in patients with atherosclerosis or vascular variations. This not only consumes time with an increased incidence rate of neurologic complications but also results in a high burden of iodinated contrast and radiation exposure.[7,9,10] Therefore, pre-DSA noninvasive vascular imaging examinations, such as CTA or contrast-enhanced MRA (CE-MRA), are crucial for the preliminary diagnosis and angioarchitecture evaluation of SVMs.[11-13] These insights can aid clinicians in optimal preoperative preparation, potentially reducing the operative duration and elevating surgical outcomes.[14,15]

Despite being radiation-free and having high tissue resolution, the use of CE-MRA for preoperative assessment is still limited because of the long scanning time, small scanning range per scan, and large contrast agent dosage, which can make it difficult for patients to remain motionless for protracted periods.[9,16] However, CTA can effectively address these issues, on the basis of its advantages of fast scanning speed for obtaining the entire range of the spine in a short time and high spatial resolution for displaying smaller subcortical blood vessels.[12] The advantages of CTA are yet to be explored further, especially in the area of vascular image postprocessing. Difficulty in simultaneous and clear display of the vertebral body and abnormal small blood vessels within the vertebral canal is the limitation of routine 3D volume rendering (3D-VR) reconstruction for SVMs.[12] On the basis of extensive clinical experience, even with meticulous bone subtraction techniques, the 3D-VR reconstruction images still have difficulty presenting the core lesions of SVMs, much less achieving a comprehensive representation of the extensively draining venous network.

This study proposes an improved 3D-VR technique, the spinal subtraction and bone background fusion CTA (SSBBF-CTA) technique, which obviates the requirement for third-party software integration. It optimizes the display of angioarchitectures of lesions and their relationship with the bones. The use of SSBBF-CTA for the accurate diagnosis and localization of SVMs can substantially assist in preoperative evaluation and clinical treatment decisions.

MATERIALS AND METHODS

Patients

Forty-nine patients, including 22 patients diagnosed with SVMs (group A) and 27 patients without SVMs (group B), between November 2017 and November 2022, were retrospectively enrolled in our study. The inclusion criteria were as follows: 1) clinical manifestations of motor/sensory disturbances; 2) all patients having undergone spinal CTA examinations, including precontrast and arterial phase (AP) imaging; 3) group A: DSA examination conducted within 1 week that confirmed the diagnosis of SVMs; and 4) group B: DSA, MR imaging, and other sufficient evidence that confirmed the absence of SVMs by clinical physicians and radiologists with >10 years of experience. The exclusion criteria were as follows: 1) insufficient or incomplete clinical data, 2) intramedullary tumors or after aortic replacement surgery, and 3) severe motion artifacts on images. The patient screening process is illustrated in the flow chart shown in Fig 1. This retrospective study received approval from the institutional review board and was granted an exemption from the requirement for informed consent.

CT Protocol

All patients underwent multiphasic CT consisting of precontrast and AP images using a Somatom Definition Flash CT scanner (Siemens). The scan parameters were as follows: 10-0kV tube voltage, tube current determined by the Automatic Tube Current Modulation system (Care Dose4D, Siemens; 100-mAs reference tube current, and 120- to 350-mAs effective tube current), 0.28-second gantry rotation time, 1.2 pitch, 64 × 0.6 mm collimation. All data sets were reconstructed with a slice thickness of 0.75 mm and an increment of 0.5 mm. The contrast agent (iomeprol, Iomeron, 400 mgI/mL; Shanghai Bracco Sine Pharmaceutical) was injected at a flow rate of 0.075 mL/kg/s, 14-second injection duration, and 10-second same flow of saline. The AP determined by the bolus-tracking technique started 8 seconds after the threshold of the ascending aorta reached 120 HU. The scanning ranges of the 2 phases were identical.

Image Postprocessing

First, all the original images, including the precontrast and AP images, were transferred to a postprocessing workstation (syngo.via VB20; Siemens), and the multiplanar reconstruction images were obtained. Routine bone subtraction CTA (RBS-CTA) 3D-VR images were obtained by subtracting the precontrast images from the AP images on the basis of the currently more precise bone subtraction algorithm of Siemens. Second, all original and RBS-CTA images were transferred to the ADW4.6 workstation (GE Healthcare), which is more proficient in the reconstruction of microvascular structures. Bone background images were obtained by reconstructing precontrast images. The aortic trunk and branches were obtained from the RBS-CTA images. Abnormal vascular structures were identified by processing the original AP images. The fusion of the 3 aforementioned types of images produced SSBBF-CTA images. The MPR images were postprocessed in real-time following patient scanning, whereas the RBS and SSBBF-CTA images were processed retrospectively.

Image Analysis and Evaluation Criteria

Three major steps were involved in image analysis. Patients were randomly assigned to each reading session. All readers read the images independently and blinded to the final diagnosis. Postprocessing image reconstruction and diagnostic accuracy were evaluated against DSA as the criterion standard, which was verified by seasoned vascular interventionalists (Online Supplemental Data).

1) Preliminary screening capability using original images with MPR-CTA to evaluate the actual diagnostic accuracy of SVMs when radiologists first read radiographs using only general images. The patients in groups A and B were randomized, and 3 types of readers 1–3 participated in this step. Reader 1 was a junior undergoing radiologist training with 1 year of experience.

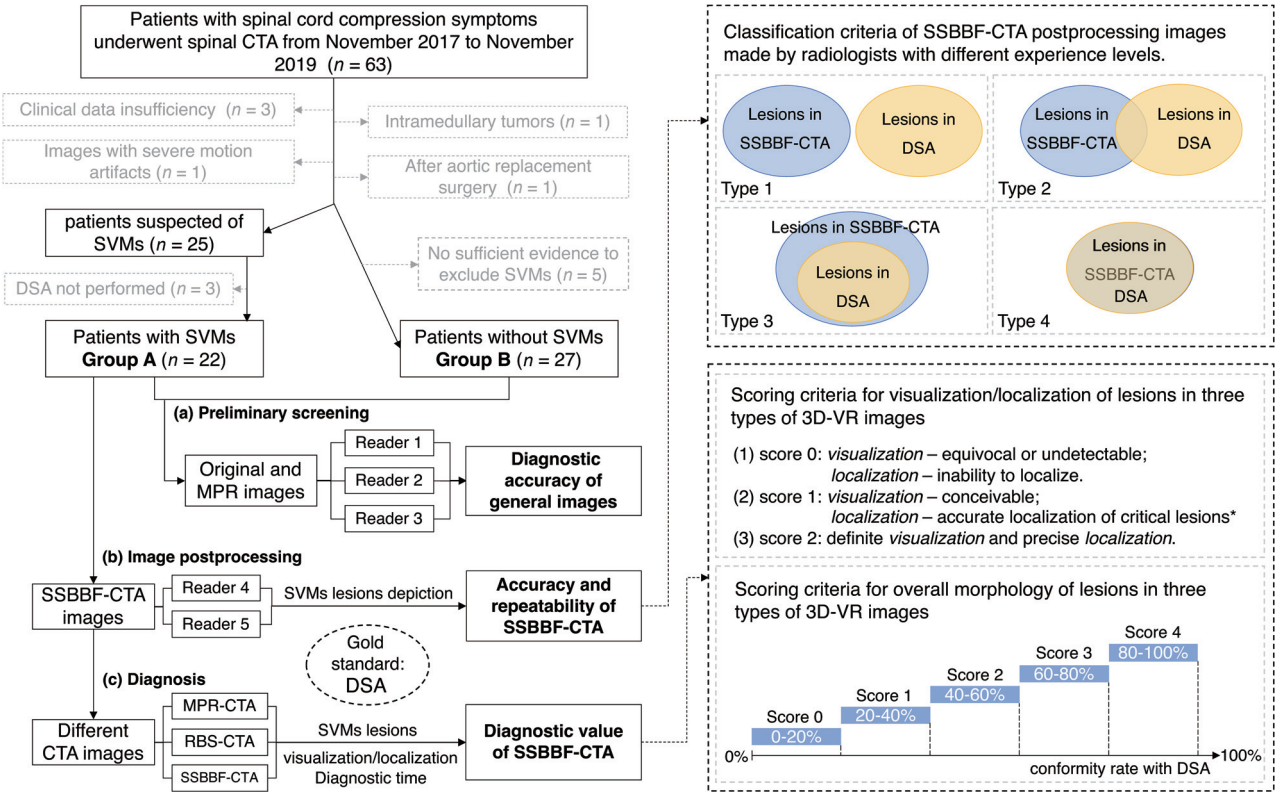

FIG 1. Flow chart of the patient enrollment process and workflow of this study. *Asterisk* indicates accurate localization of critical lesions which defined as mostly correct when multiple feeding arteries are present, and the identification of drainage veins covering over 70% of the range.

Reader 2 was a type of junior practicing radiologist with 3–8 years of experience, who submitted the original diagnostic report for the first time. Reader 3 was a type of senior radiologist with >10 years of experience who signed the report.

2) The accuracy and stability of the SSBBF-CTA postprocessing technique to evaluate whether the postprocessing method of SSBBF-CTA performed by radiologists with different experience levels was accurate and repeatable. Images of group A were used. The SSBBF-CTA image postprocessing was performed by 2 practicing radiologists with 4 and 20 years of experience (readers 4 and 5, respectively), and the differences between the 2 were assessed. The classification criteria (types 1–4) of SSBBF-CTA images are shown in Fig 1, including the localization and number of nidus/fistulas and feeding arteries, the extent of the drainage vein, and overall morphology.

3) Diagnostic value of lesion details of SVMs using 3 types of postprocessing images to analyze the lesion details (visualization and localization of feeding arteries, nidus/fistula, and draining veins) by different 3D-VR images and compare the differences among the 3. Reader 1 (same as above) and reader 4 evaluated and scored the lesions of SVMs in the MPR-CTA, RBS-CTA, and SSBBF-CTA images, respectively. All final scores were confirmed by discussion in cases of disagreement and supervised by reader 5. Finally, a comparison of the diagnostic time was made between reader 1 and reader 4 in terms of evaluating all SVM lesions using MPR-CTA and SSBBF-CTA. The scoring criteria for the visualization/localization of lesions (evaluating feeding arteries, nidus, and draining veins separately) and overall morphology in MPR, RBS, and SSBBF-CTA images are shown in Fig 1.

Statistical Analysis

Demographic and clinical variables were compared between patients in groups A and B. The Mann-Whitney *U* test was used for non-normally distributed quantitative data. For normally distributed data, the independent samples *t* test was used. χ^2 tests were performed on categoric data. Receiver operating characteristic (ROC) analysis was performed to evaluate the diagnostic performance of readers 1–3, using DSA diagnosis as the criterion standard. Comparison of the areas under the ROC curves was performed using the DeLong test. The Wilcoxon signed-rank test was used to compare the differences between the postprocessed images of readers 4 and 5, as well as the differences in diagnostic evaluation and time between readers 1 and 4. The Kruskal-Wallis rank sum test was used to compare the differences in lesion identification and localization among the different postprocessing images.

All continuous variables were expressed as mean (SD) when normally distributed and median (interquartile range) if not. Statistical significance was set at $P < .05$. Statistical analyses were performed using SPSS (Version 25.0; IBM) and MedCalc (Version 18.21.1; MedCalc Software).

RESULTS

Patient Characteristics

Of 63 patients with similar symptoms of spinal cord compression who underwent preoperative spinal CTA, 14 were excluded from this study for the following reasons: 1) insufficient clinical data

($n = 3$); 2) patients with intramedullary tumors ($n = 1$) or aortic replacement surgery ($n = 1$); 3) images with severe motion artifacts ($n = 1$); 4) patients suspected of having SVMs without confirmed DSA ($n = 3$); and 5) no sufficient evidence to exclude patients with SVMs ($n = 5$). Accordingly, 49 patients (group A: 22 patients; mean age, 44.0 [SD, 14.3] years; and group B: 27 patients; mean age 44.6 [SD, 15.2] years) comprised the final study sample, and their demographic and clinical variables are summarized in Table 1. Only urogenital disturbances showed statistically significant differences between patients with and without SVMs ($P = .005$).

Preliminary Screening of SVMs

The diagnostic efficacies of the original images with MPR for the primary screening of SVMs by different readers are shown in Table 2. As radiologic experience increased, the area under the curve (AUC) values for readers 1, 2, and 3 were 0.849, 0.936, and 0.977, respectively. Among all diagnostic indicators, sensitivity was the least effective, with reader 1 demonstrating a sensitivity of only 77.3%. Moreover, the DeLong test demonstrated a statistically significant difference between the ROC curves of reader 1 and reader 3 ($P = .031$).

SSBBF-CTA Postprocessing Images

The SSBBF-CTA images processed by readers 4 and 5 were classified into 4 types: types 1–4. The higher the classification level, the greater was the clinical utility, with types 3 and 4 being considered particularly beneficial in aiding clinical diagnosis and treatment. Nearly all lesion characteristics, including localization and the number of nidi/fistulas, drainage veins, and overall morphology, were classified as either type 3 or 4, with the majority falling into the type 4 category (Fig 2). Only 2 cases had deviations in the feeding artery, characterized by the presence of multiple supplying vessels or the involvement of complex scenarios involving the extracranial arteries and intracranial collateral circulation (Online Videos 1 and 2). In addition, no statistically significant difference was observed between readers 4 and 5 ($P > .05$).

Table 1: Patient characteristics[a]

	Group A	Group B	*P* Value
Age (yr)[b]	44.0 (SD, 14.3)	44.6 (SD, 15.2)	.898
Sex[c]			.990
Female	9	11	
Male	13	16	
Sensory disturbance	100% (22/22)	88.9% (24/27)	.242
Motor disturbance	90.9% (20/22)	77.8% (21/27)	.269
Reflex abnormality	68.2% (15/22)	66.7% (18/27)	.910
Urogenital disturbance	72.7% (16/22)	33.3% (9/27)	.005[d]
Back pain	9.1% (2/22)	11.1% (3/27)	1.000

[a] Unless otherwise indicated, data are percentages, with numbers of patients in parentheses.
[b] Age is presented as the mean.
[c] Data are numbers of patients.
[d] The clinical features of groups A and B showed statistically significant differences ($P < .05$).

Diagnosis and Evaluation of SVMs Using Different CTA Postprocessing Images

We compared the diagnostic capabilities of SVM lesions using 3 postprocessing methods (MPR-CTA, RBS-CTA, and SSBBF-CTA, Figs 3 and 4, Online Videos 3 and 4), using scores that were discussed by readers 1 and 4 and subsequently corrected under the supervision of reader 5. In terms of accuracy in visualization and localization of lesions (nidus/fistula, feeding artery, and drainage vein) and the overall morphology of SVMs, RBS-CTA demonstrated significantly inferior performance ($P = .000$) compared with MPR-CTA and SSBBF-CTA, whereas no significant difference ($P > .05$) was observed between MPR and SSBBF (Table 3). Additionally, reader 1 performed worse than reader 4 in the assessment of lesions using MPR-CTA ($P < .05$), whereas no difference ($P > .05$) was observed between the 2 when using SSBBF-CTA (Table 4 and Online Supplemental Data). Moreover, both readers 1 and 4 required significantly less diagnostic time when using SSBBF-CTA for lesion assessment than when using MPR-CTA ($P = .000$, Table 4).

DISCUSSION

This study used clinically prevalent postprocessing workstations to optimize postprocessing techniques for spinal artery CTA, achieving precise visualization and localization of SVM lesions using 3D-VR, thereby enhancing the diagnostic ability and efficiency of radiologists. This advancement allows clear visualization of tertiary and higher-order arterial branches within 3D-VR images, potentially having considerable importance for the diagnostic utility of CTA in vasculopathy.

The accuracy of SVM diagnosis using the original and MPR-CTA images was lower for junior physicians than for more experienced physicians, particularly in terms of diagnostic sensitivity. The incidence rate of SVMs was quite low, making it impractical to reach an occurrence rate of approximately 50% in this study. Therefore, in the practical field of radiology, the likelihood of diagnostic errors or missed diagnoses is even higher.[17] However, the consequences of a missed diagnosis or misdiagnosis can be very serious for patients with SVMs.[4] Impairment of spinal cord venous drainage can result in progressive neurologic deficit symptoms, such as sensory, motor, and even urogenital disturbances, which lead to disability and significantly impact the patient's

Table 2: Diagnostic efficacy of original images with MPR for primary screening of SVMs by different readers[a]

Reader	Sensitivity (%)	Specificity (%)	Accuracy (%)	PPV (%)	NPV (%)	AUC [95% CI]	Youden
Reader 1[b]	77.3 (17/22)	92.6 (25/27)	85.7 (42/49)	89.5 (17/19)	83.3 (25/30)	0.849 (0.718–0.935)	0.699
Reader 2	90.9 (20/22)	96.3 (26/27)	93.9 (46/49)	95.2 (20/21)	92.9 (26/28)	0.936 (0.828–0.986)	0.872
Reader 3	95.5 (21/22)	100 (27/27)	98.0 (48/49)	100 (21/21)	96.4 (27/28)	0.977 (0.888–0.999)	0.955

Note:—PPV indicates positive predictive value; NPV, negative predictive value; Reader 1, a radiologist with one year of experience; Reader 2, a junior physician who submitted the original report for the first time;Reader 3, a reviewing physician who also submitted the original report for the first time.
[a] Data in brackets are 95% CIs, and data in parentheses are numbers of patients.
[b] Readers 1 and 3 showed statistically significant differences ($P < .05$).

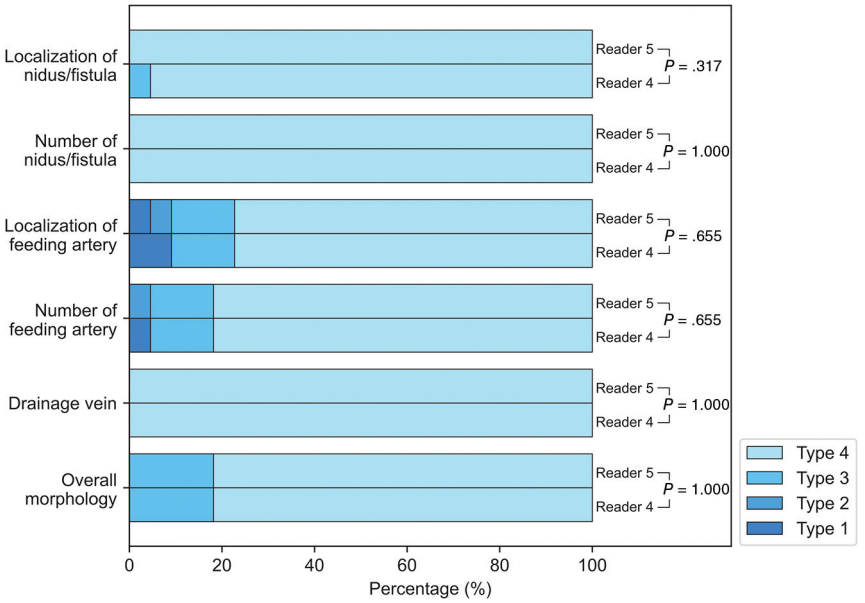

FIG 2. Percentage of stacked bar chart of categorization of postprocessing SSBBF reconstruction accuracy. Types 3 and 4 are considered particularly beneficial in aiding clinical diagnosis and treatment.

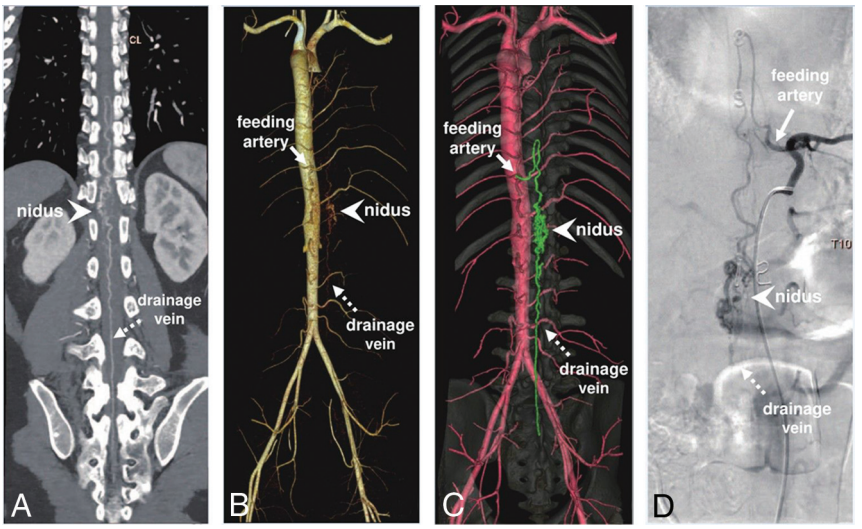

FIG 3. Spinal CTA images in a 28-year-old man with a spinal AVM. The crucial lesions, including nidus (*arrowhead*), feeding artery (*solid arrow*), and drainage vein (*dotted arrow*), are shown in MPR-CTA (*A*), RBS-CTA (*B*), SSBBF-CTA (*C*), and DSA images (*D*).

quality of life.[18-20] If misdiagnosed as a demyelinating disease, treatment with hormone shock therapy may lead to hematomyelia, which can be fatal.[21,22] Therefore, improving the diagnostic sensitivity of pretreatment patient screening can reduce potentially serious medical risks. We recommend that the following patients should undergo CTA examination with our SSBBF-CTA method before treatment after balancing radiation and clinical needs: 1) those presenting with special neurologic symptoms, 2) those with an initial MRI suggesting evident flow void signals adjacent to the spinal cord, 3) those with existing examinations that could not definitively rule out vascular anomalies, and 4) those with contraindications for MR imaging and no contraindications for CTA.

This study achieved clear visualization and localization of SVM lesions by innovatively combining the advantages of Siemens and GE Healthcare postprocessing workstations for image postprocessing without the need for third party software. The spinal artery, a third-order or higher branch with a small diameter, runs through the intervertebral foramen and spinal canal and is closely related to the vertebrae.[23] These unique anatomic features make it challenging to maintain vessel continuity while accurately subtracting the bones. According to our clinical experience, the bone subtraction algorithm of the Siemens workstation is more precise,[24] but it falls short of displaying the small vessels of SVMs. The GE Healthcare workstation can display complete SVMs lesion details by tracking small vessels; however, it cannot obtain clean aorta and intercostal artery 3D-VR images using its bone subtraction algorithm. Thus, a combination of the advantages of both workstations provided clear and unobstructed 3D-VR reconstruction images of the SVMs. The fusion of a reduced-opacity bone background with clear vessels was implemented to achieve accurate localization of the SVM lesion without obstructing their visibility. A spinal CTA acquisition (from the beginning of the noncontrast scan to the completion of the CTA) rarely exceeds 1 minute and, therefore, rarely produces motion artifacts. Because the positioning coordinates of the images in the plain scan and APs are consistent and the image superposition is based on the coordinates, no additional artifacts will affect the image quality. Furthermore, junior physicians can achieve a level of accuracy in SSBBF-CTA images comparable with that of experienced physicians through short-term training, and the difference in the amount of time required to perform postprocessing was minimal. However, in complex cases, it is advisable to perform these procedures under the supervision of experienced physicians.

Preoperative information regarding the nidi/fistulas, feeding arteries, and drainage veins of SVMs is crucial for guiding the selection of clinical treatment plans. When using MPR-CTA, the less experienced physicians tended to have a lower accuracy than the physicians with more extensive experience, and both physicians demonstrated high accuracy in evaluating SVM lesions when using SSBBF-CTA. This finding indicates that the use of the

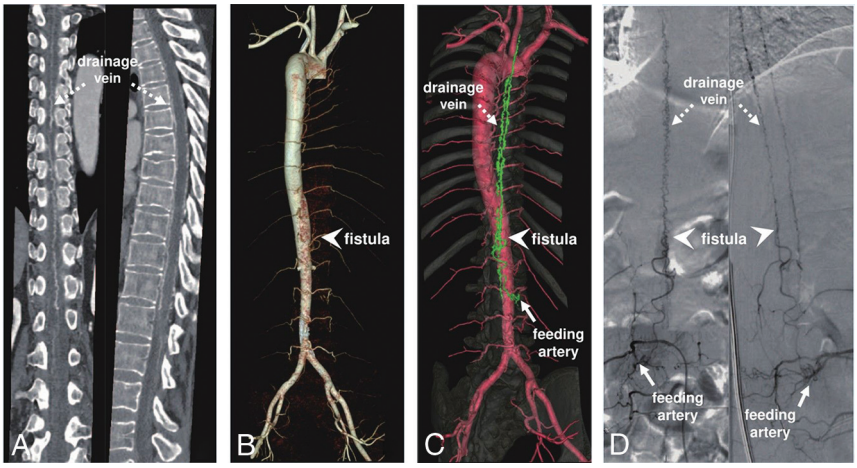

FIG 4. Spinal CTA images in a 55-year-old woman with a spinal AVF. The crucial lesions, including the fistula (*arrowhead*), feeding artery (*solid arrow*), and drainage vein (*dotted arrow*), are shown in an MPR-CTA image (*A*), a RBS-CTA image (*B*), SSBBF-CTA image (*C*), and a DSA image (*D*).

Table 3: Scoring of lesion localization and visualization of SVMs using different postprocessing techniques of CTA images[a]

	MPR-CTA	RBS-CTA[b]	SSBBF-CTA	*P* Value[c]
Visualization of lesions (total points)	6.00 (1.00)	4.00 (2.75)	6.00 (0.63)	.000
Nidus/fistula	2.00 (0.00)	1.50 (1.00)	2.00 (1.25)	.000
Feeding artery	2.00 (0.63)	1.00 (1.50)	2.00 (0.00)	.000
Drainage vein	2.00 (0.00)	1.00 (1.00)	2.00 (0.00)	.000
Localization of lesions (total points)	6.00 (0.00)	3.25 (3.00)	6.00 (1.00)	.000
Nidus/fistula	2.00 (0.00)	1.00 (1.00)	2.00 (0.00)	.000
Feeding artery	2.00 (0.00)	1.00 (2.00)	2.00 (0.00)	.000
Drainage vein	2.00 (0.00)	1.00 (1.13)	2.00 (0.00)	.00
Overall morphology	4.00 (0.00)	2.75 (2.63)	4.00 (0.50)	.000

[a] The data are presented as median (interquartile range).
[b] There is a statistically significant difference between RBS-CTA and the other 2 groups ($P < .05$).
[c] There is a significant statistical difference among the 3 groups ($P < .05$).

Table 4: Assessment of lesions of SVMs and diagnostic time using different postprocessing CTA techniques by different readers[a]

	Reader 1	Reader 4	*P* Value
MPR-CTA			
Visualization of lesions	4.00 (1.25)	6.00 (1.00)	.001[b]
Localization of lesions	4.50 (2.00)	6.00 (0.00)	.003[b]
Overall morphology	4.00 (1.00)	4.00 (0.00)	.025[b]
Diagnostic time	9.00 (6.75)	7.00 (3.00)	.017[b]
RBS-CTA			
Visualization of lesions	3.50 (3.00)	3.50 (3.00)	.353
Localization of lesions	2.25 (3.00)	3.00 (2.50)	.178
Overall morphology	2.50 (1.25)	3.00 (2.00)	.070
Diagnostic time	NA	NA	NA
SSBBF-CTA			
Visualization of lesions	6.00 (1.00)	6.00 (1.00)	.705
Localization of lesions	6.00 (1.00)	6.00 (1.00)	.206
Overall morphology	4.00 (0.25)	4.00 (0.13)	.655
Diagnostic time	3.00 (2.00)[c]	3.00 (1.25)[c]	.943

Note:—NA indicates not applicable; Reader 1, a radiologist with one year of experience; Reader 4, a radiologist with 4 years of experience.
[a] The data are presented as median (interquartile range). The visualization and localization of lesions represent the total score of the nidus/fistula, feeding artery, and drainage vein.
[b] There is a significant statistical difference between readers 1 and 4 ($P < .05$).
[c] There is a statistically significant difference in diagnostic time between the use of MPR-CTA and SSBBF-CTA ($P = .000$).

SSBBF-CTA 3D-VR reconstruction technique enables the accurate identification of the key lesions of SVMs by less-experienced radiologists and clinical physicians with limited radiologic experience. Furthermore, SSBBF-CTA can significantly shorten the diagnostic time without compromising diagnostic accuracy for both junior and senior radiologists. These aspects contribute to the establishment of effective communication between the clinical and radiology departments, thereby improving diagnostic efficiency.

The advantages of CTA have yet to be fully explored and improved. Several studies have reported that 320-layer and 640-layer spiral CTA can achieve an accuracy rate of 62.5%–85.7% in locating the fistula of spinal AVFs.[12,13,25] Our research aimed to update the postprocessing image quality on the basis of standard CTA, producing a more intuitive and clearer visualization of lesions and allowing a detailed and efficient analysis of lesion features of SVMs. 3D-VR images of types 3 and 4 were considered clinically acceptable diagnostic results, accounting for nearly 100% of the cases. The current research indicates that the accuracy of CE-MRA in locating fistulas for AVFs is higher than 80%,[26] while time-resolved CE-MRA has an even higher accuracy rate of up to 91%.[11] Therefore, in clinical practice, a reasonable selection should be made on the basis of the individual patient and hardware conditions of different hospitals, considering the respective advantages of CTA and MRA.

In addition, the classification of SVMs is complex, and at least 5 classification methods are currently known.[27] Regardless of the classification standard, there are great advantages for extramedullary high-flow lesions, such as lesions classified as type I (dural AVF) and type IV (perimedullary AVF). For intramedullary lesions (type II, intramedullary glomus AVM and type III, intramedullary juvenile AVM), CTA can also provide useful information on vascular lesions, but it is limited in the evaluation of the spinal cord. For type V, extradural AVF, it may be difficult to visualize a fistula (too closely related to the bones). Challenges remain for lesions with slow flow; however, some abnormal vascular manifestations can suggest the diagnosis of SVMs.[28] A second, late arterial CTA scan can also solve a part of this problem; however, the radiation dose issue needs to be considered.

This study has some limitations. By using SSBBF-CTA for comprehensive preoperative assessment of SVMs, clinicians can obtain more lesion details to develop appropriate surgical strategies, which can potentially shorten the surgical duration, reduce contrast agent use, and limit radiation exposure. However, the

assumption that CTA might indirectly enhance surgical outcomes remains speculative and warrants further longitudinal observation. Although the SSBBF-CTA postprocessing technology itself does not add additional radiation, CTA examinations still need to be reasonably selected by balancing radiation and patient conditions. In addition, because of the low incidence rate of the disease, the number of included patients was relatively insufficient, and this study explored only the universal applicability of SSBBF-CTA for SVMs. Our team is continuing to collect cases for a more detailed classification to further explore the practicality of SSBBF-CTA. This research methodology has been integrated into the general work of our hospital and has already helped avoid many medical risks. A one-stop image postprocessing reconstruction software that can combine the advantages of algorithms from 2 different postprocessing workstations will make clinical work more convenient. The rapid advancement of artificial intelligence technology holds great potential for achieving simplified and increasingly accurate CTA reconstruction images in the future.

CONCLUSIONS

The SSBBF-CTA technique demonstrated excellent reproducibility, significantly enhancing both the accuracy and efficiency of the diagnosis and assessment of SVMs, with particular benefits for junior radiologists. It has the potential for substantial clinical benefits in the preoperative evaluation and selection of appropriate treatment strategies.

Disclosure forms provided by the authors are available with the full text and PDF of this article at www.ajnr.org.

REFERENCES

1. Clarencon F, Di Maria F, Sourour NA, et al. **Evaluation of intra-aortic CT angiography performances for the visualisation of spinal vascular malformations' angioarchitecture**. *Eur Radiol* 2016;26:3336–44 CrossRef Medline
2. Zalewski NL, Rabinstein AA, Brinjikji W, et al. **Unique gadolinium enhancement pattern in spinal dural arteriovenous fistulas.** *JAMA Neurol* 2018;75:1542–45 CrossRef Medline
3. Jeng Y, Chen DY, Hsu HL, et al. **Spinal dural arteriovenous fistula: imaging features and its mimics.** *Korean J Radiol* 2015;16:1119–31 CrossRef Medline
4. Yu JX, Hong T, Krings T, et al. **Natural history of spinal cord arteriovenous shunts: an observational study.** *Brain* 2019;142:2265–75 CrossRef Medline
5. Hunt R, Roberts RM, Mortimer AM. **Spinal dural arteriovenous fistula: delay to radiological diagnosis and sources of radiological error.** *Clin Radiol* 2018;73:835.e811–e816 CrossRef Medline
6. Jablawi F, Schubert GA, Dafotakis M, et al. **Long-term outcome of patients with spinal dural arteriovenous fistula: the dilemma of delayed diagnosis.** *AJNR Am J Neuroradiol* 2020;41:357–63 CrossRef Medline
7. Orru E, Mekabaty AE, Millan DS, et al. **Removal of antiscatter grids for spinal digital subtraction angiography: dose reduction without loss of diagnostic value.** *Radiology* 2020;295:390–96 CrossRef Medline
8. Barreras P, Heck D, Greenberg B, et al. **Analysis of 30 spinal angiograms falsely reported as normal in 18 patients with subsequently documented spinal vascular malformations.** *AJNR Am J Neuroradiol* 2017;38:1814–19 CrossRef Medline
9. Tarabishy AR, Boo S, Rai A. **Spinal dural fistula evaluation using 4-dimensional intra-aortic spinal CT angiography in a hybrid angiography suite.** *J Neuroradiol* 2021;48:492–94 CrossRef Medline
10. Lee CW, Huang A, Wang YH, et al. **Intracranial dural arteriovenous fistulas: diagnosis and evaluation with 64-detector row CT angiography.** *Radiology* 2010;256:219–28 CrossRef Medline
11. Grossberg JA, Howard BM, Saindane AM. **The use of contrast-enhanced, time-resolved magnetic resonance angiography in cerebrovascular pathology.** *Neurosurg Focus* 2019;47:E3 CrossRef Medline
12. Kim AY, Khil EK, Choi I, et al. **Spinal extradural arteriovenous fistula after lumbar epidural injection: CT angiographic diagnosis using 3D-volume rendering.** *Skeletal Radiol* 2020;49:2073–79 CrossRef Medline
13. Brinjikji W, Colombo E, Cloft HJ, et al. **Clinical and imaging characteristics of spinal dural arteriovenous fistulas and spinal epidural arteriovenous fistulas.** *Neurosurgery* 2021;88:666–73 CrossRef Medline
14. Lai PH, Weng MJ, Lee KW, et al. **Multidetector CT angiography in diagnosing type I and type IVA spinal vascular malformations.** *AJNR Am J Neuroradiol* 2006;27:813–17 Medline
15. Yamamoto S, Kanaya H, Kim P. **Spinal intraarterial computed tomography angiography as an effective adjunct for spinal angiography.** *J Neurosurg Spine* 2015;23:360–67 CrossRef Medline
16. Kannath SK, Rajendran A, Thomas B, et al. **Volumetric T2-weighted MRI improves the diagnostic accuracy of spinal vascular malformations: comparative analysis with a conventional MR study.** *J Neurointerv Surg* 2019;11:1019–23 CrossRef Medline
17. Ronald AA, Yao B, Winkelman RD, et al. **Spinal dural arteriovenous fistula: diagnosis, outcomes, and prognostic factors.** *World Neurosurg* 2020;144:e306–15 CrossRef Medline
18. Zhang HB, Zhai XL, Li L, et al. **Imaging characteristics, misdiagnosis and microsurgical outcomes of patients with spinal dural arteriovenous fistula: a retrospective study of 32 patients.** *Ann Transl Med* 2022;10:832 CrossRef Medline
19. Naylor RM, Topinka B, Rinaldo L, et al. **Progressive myelopathy from a craniocervical junction dural arteriovenous fistula.** *Stroke* 2021;52:e278–81 CrossRef Medline
20. Jablawi F, Mull M. **The clinical value of venous drainage in patients with spinal dural arteriovenous fistula.** *J Neurol Sci* 2019;397:50–54 CrossRef Medline
21. Donghai W, Ning Y, Peng Z, et al. **The diagnosis of spinal dural arteriovenous fistulas.** *Spine (Phila Pa 1976)* 2013;38:E546–53 CrossRef Medline
22. Ma Y, Hong T, Chen S, et al. **Steroid-associated acute clinical worsening and poor outcome in patients with spinal dural arteriovenous fistulas: a prospective cohort study.** *Spine (Phila Pa 1976)* 2020;45:E656–62 CrossRef Medline
23. Hsu JL, Cheng MY, Liao MF, et al. **The etiologies and prognosis associated with spinal cord infarction.** *Ann Clin Transl Neurol* 2019;6:1456–64 CrossRef Medline
24. Aulbach P, Mucha D, Engellandt K, et al. **Diagnostic impact of bone-subtraction ct angiography for patients with acute subarachnoid hemorrhage.** *AJNR Am J Neuroradiol* 2016;37:236–43 CrossRef Medline
25. Shimoyama S, Nishii T, Watanabe Y, et al. **Advantages of 70-kV CT angiography for the visualization of the Adamkiewicz artery: comparison with 120-kV imaging.** *AJNR Am J Neuroradiol* 2017;38:2399–405 CrossRef Medline
26. Lindenholz A, TerBrugge KG, van Dijk JM, et al. **The accuracy and utility of contrast-enhanced MR angiography for localization of spinal dural arteriovenous fistulas: the Toronto experience.** *Eur Radiol* 2014;24:2885–94 CrossRef Medline
27. Deng F, Knipe H. **Spinal vascular malformations.** 2016. *Radiopaedia* Radiopaedia.org. Accessed October 18, 2023
28. Kona MP, Buch K, Singh J, et al. **Spinal vascular shunts: a patterned approach.** *AJNR Am J Neuroradiol* 2021;42:2110–18 CrossRef Medline